

Comparative study on bearing characteristics of pervious concrete piles in silt and clay foundations

Jun Cai^{1a}, Guangyin Du^{*2}, Han Xia¹ and Changshen Sun²

¹School of Transportation, Southeast University, Jiulong Lake Campus, P.R. China

²Zhejiang Provincial Institute of Communications Planning, Design and Research, Westlake district, P.R. China

(Received August 31, 2021, Revised October 18, 2021, Accepted November 10, 2021)

Abstract. With the advantages of high permeability and strength, pervious concrete piles can be suitable for ground improvement with high water content and low bearing capacity. By comparing the strength and permeability of pervious concrete with different aggregate sizes (3-5 mm and 4-6 mm) and porosities (20%, 25%, 30% and 35%), the recommended aggregate size (3-5 mm) and porosity (30%) can be achieved. The model tests of the pervious concrete piles in soft soil (silt and clay) foundations were conducted to evaluate the bearing characteristics, results show that, for the higher consolidation efficiency of the silty foundation, the bearing capacity of the silty foundation is 16% higher, and the pile-soil stress ratio is smaller. But when it is the ultimate load for the piles, they will penetrate into the underlying layer, which reduces the pile-soil stress ratios. With higher skin friction of the pile in the silty foundation, the pile penetration is smaller, so the decrease of the pile axial force can be less. For the difference in consolidation efficiency, the skin friction of pile in silt is more affected by the effective stress of soil, while the skin friction of pile in clay is more affected by the lateral stress. When the load reaches 4400 N, the skin friction of the pile in the silty foundation is about 35% higher than that of the clay foundation.

Keywords: bearing characteristic; clay foundation; model test; pervious concrete pile; silt foundation

1. Introduction

With the development of city construction, the requirement for the treatment of soft soils is upgrading, the most commonly used ground-improvement technique in soft soil foundation is permeable granular columns (Andreou *et al.* 2008), which can be utilized to improve soil strength and provide a drainage path. The permeable granular columns mainly include sand compaction piles (Kwon *et al.* 2018, Ahn and Kim 2012) and stone columns (Yu *et al.* 2020). Obviously, the permeable granular columns could increase the time rate of consolidation, improve bearing capacity, and reduce settlement (Mitchell 1981, Barksdale and Bachus 1983, Baez 1995, Okamura *et al.* 2006). But compared with other piles with high strength, the quality of granular columns is lower and more affected by the properties of the surrounding soil (Alamgir *et al.* 1996, Andreou *et al.* 2008). Therefore, the applications of granular columns in very soft clays and silts were limited. So a kind of material with high strength and permeability was noted for the application of the treatment on poor soils, it is the pervious concrete, which has been widely used in pavement due to its storm runoff capabilities, rain wastewater control and acoustic absorption (Tennis *et al.* 2004, Neithalath *et al.* 2010). It is a special kind of concrete with a little amount of fines or no fines, so

the continuous pores could drain away water (Ghafoori *et al.* 1995, Schokker 2010, Qin *et al.* 2016). Pervious concrete is a mixture of narrowly graded coarse aggregates, cement and water, which forms an interconnected macro pore internal matrix (Huang *et al.* 2010, Yahia and Kabagire 2014, ACI 2010), resulting in a very pores structure. Besides, the compressive strength of pervious concrete can be 2.8-28 MPa (Malaiskiene *et al.* 2020), and the permeability coefficient is generally 2.0-5.4 mm/s, even some can reach 12 mm/s (Tennis *et al.* 2004). Suleiman *et al.* (2014) and Ni *et al.* (2016) developed a new ground-improvement method using pervious concrete piles, which are capable of improving foundations with high water content, and reduce the settlement and liquefaction of ground. Also, the performance of pervious concrete piles under vertical and lateral loads, and the influence of installation method of the pervious concrete pile were compared. The research group of Cui (Cui *et al.* 2012, Zhang *et al.* 2013, Zhang *et al.* 2016, Cui *et al.* 2018) investigated the dynamic performance of pervious concrete pile composite foundation during the earthquake, and found that the dissipation of excess pore water pressure was the fastest, concluded that the pervious concrete pile is particularly suitable for the reinforcement of foundation with low strength and poor permeability.

Above all, a lot of research about the seismic and liquefaction resistance of pervious concrete piles have been conducted, but the bearing characteristics of pervious concrete pile composite foundation are still in the initial stage, especially for the soft soil foundations, which can be necessary for its application in highway facilities constructed on poor soils (Fig. 1). In this study, the model test method was utilized to reveal the different bearing characteristics of the pervious concrete pile in silty and clay foundations.

*Corresponding author, Professor

E-mail: guangyin@seu.edu.cn

^aPh.D.

E-mail: caijun129@seu.edu.cn

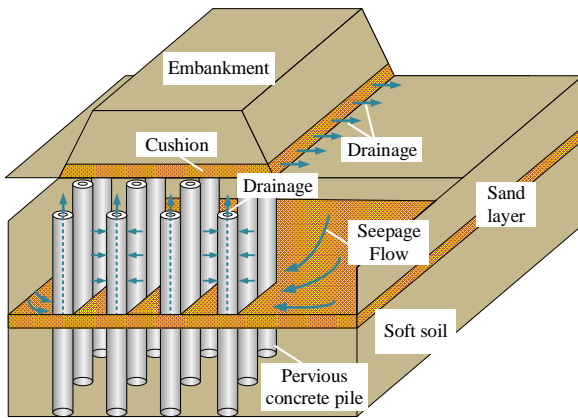


Fig. 1 Schematic of the application of the pervious concrete piles

Table 1 Test schemes of the pervious concrete preparation

Step number	Procedure	Step number	Procedure
1	Aggregate size and porosity design	5	Compressive strength and permeability test
2	Mix proportions calculation	6	Test results comparison
3	Mixing of pervious concrete ingredients	7	Pervious concrete parameter selection
4	Specimens preparation and maintenance	8	Model pervious concrete pile preparation

Table 2 Physical parameters of aggregates

Particle size(mm)	Specific gravity	Compacted stacking density (g/cm ³)	Porosity (%)
3-5	2.632	1.587	39.7
4-6	2.857	1.639	42.6

2. Preparation of pervious concrete

For the cast-in-place pile, the quality of the pile can be influenced by complex environmental factors, so the model pile in this test was set to be the precast pile. The test schemes of the model pervious concrete pile preparation are presented in Table 1. For the preparation of pervious concrete, limestone was used as the aggregate, and two kinds of particle sizes (3-5 mm and 4-6 mm) were available, the parameters for the aggregates are in Table 2.

According to the technical specification of CJJ/T 135-2009 for the pervious concrete pavement, the strength grade of cement should be 42.5 or above it, so high-grade cement (P.O. 52.5) was applied in the test. Considering the early strength property of the cement and economy, the mixture mainly includes aggregates, cement and water, without accelerator and additives.

The mix proportions of the pervious concrete were achieved from the Eq. (1)

$$\frac{m_g}{\rho_g} + \frac{m_c}{\rho_c} + \frac{m_w}{\rho_w} + p = 1 \quad (1)$$

Table 3 Mix proportions per cubic meter of the pervious concrete

Aggregate size (mm)	Target porosity (%)	Aggregate (kg)	Cement (kg)	Water (kg)
3-5	20	1 555	500	150
	25		380	114
	30		261	78
	35		141	42
4-6	20	1 606	567	170
	25		447	134
	30		328	98
	35		208	62

Table 4 Mixing procedure

Procedure	
Step 1	Mix the aggregate and 50%-60% water
Step 2	Mix together for 3 minutes
Step 3	Add cement and the rest water
Step 4	Mix thoroughly for 30 s
Step 5	Discharge

where m_g , m_c , m_w , are the amount of aggregate, cement and water per unit volume (kg/m³); ρ_g , ρ_c , ρ_w are the density of aggregate, cement and water (kg/m³); P is the designed porosity (%). According to the results of ACI (ACI 2010) and the size of the model box, the aggregate sizes in the test can be 3-5 mm and 4-6 mm, and the porosities can be 20%, 25%, 30% and 35%. The mix proportion of the pervious concrete per unit volume can be obtained from Eq. (1), and the results are shown in Table 3. Besides the mixing procedure is also important for the properties of pervious concrete, and it is in Table 4, the specimens of pervious concrete are in Figs. 2(a)-2(h).

In order to acquire the recommended mix ratio of the pervious concrete, the 28-day uniaxial compressive strength and permeability of pervious concrete were tested. The water permeability of a material is defined as its ability to pass through the water under the effect of a pressure gradient (Nguyen *et al.* 2014). It is better to apply the constant water head method to determine the material with higher permeability (D2434-74), so in this test, the permeability coefficient was acquired as a constant head. The glue was applied around the side of the specimens to make them enclosed in the transparent pipe, as shown in Fig. 3. Repeat the test 3 times, and take the average of the results, the permeability coefficient is got by

$$k_T = \frac{QL}{AHt} \quad (2)$$

where k_T is the permeability coefficient at T °C, Q is the average volume of water outflow for 5 minutes, L is the thickness of the specimen, A is the drainage area of a specimen, H is the water head difference and t is the recording time.

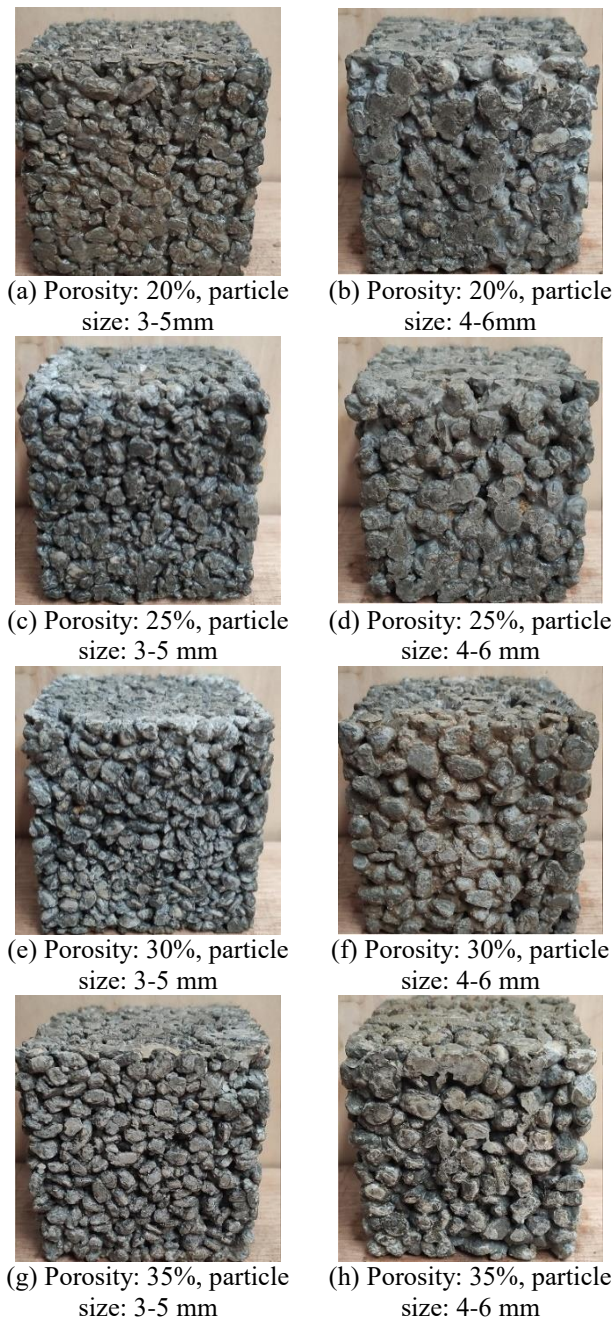


Fig. 2 Pervious concrete specimens

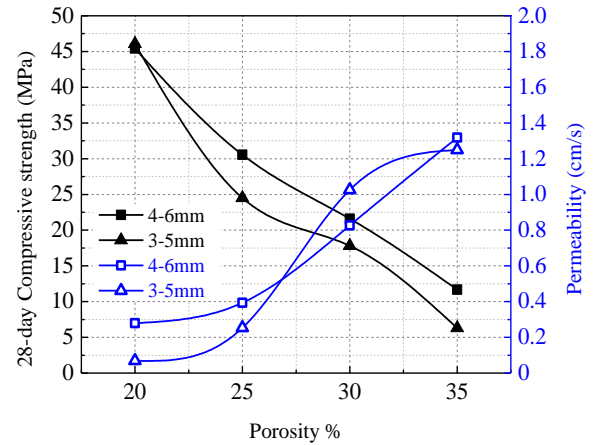


Fig. 4 Compressive strength and permeability of pervious concrete using different aggregate sizes and porosities

The permeability coefficient is influenced by water head difference (Tao 2006), and it is got by Darcy’s relationship is valid in the laminar flow regime (Das 2010), so the hydraulic gradient is set to be 0.3. Besides the uniaxial compressive strength of pervious concrete was tested (Fig. 3(b)), and the average strength and permeability coefficient with different porosities are in Fig. 4. In most cases, the failure of the composite foundation is not on the pile with high strength, but the pile-soil contact surface. So in the premise of the strength satisfaction, the pervious concrete with higher permeability can be acceptable. For both strength and permeability, the aggregate size of pervious concrete can be 3-5 mm, with the porosity being 30%.

3. Installation of model test

3.1 Model pile and test facility

Loading test is the most effective method to determine the bearing capacity of the composite foundation, and the bearing characteristics of composite foundation under vertical load can be convincing (Zhang *et al.* 2014), the test schemes of the vertical load test are presented in Table 5.

According to the technical code of DB37/T 5214-2018 for the composite foundation of the pervious concrete pile, the diameter of the pile in-site is recommended as 300-500

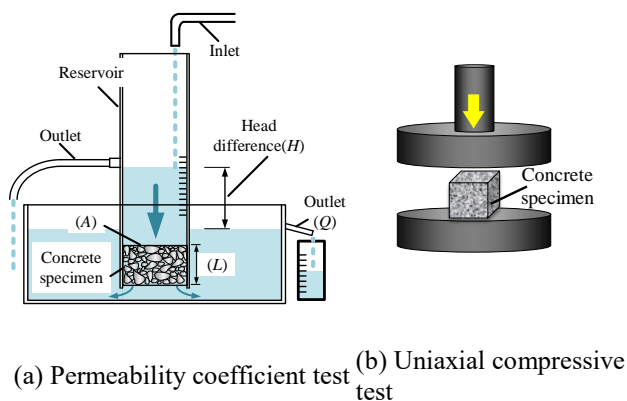


Fig. 3 Laboratory tests of pervious concrete specimens

Table 5 Test schemes of the vertical load test

Step number	Procedure	Step number	Procedure
1	Parameter design of composite foundation	5	Cushion arrangement
2	Foundation soil preparation	6	Preloading and unloading
3	Foundation soil filling and sensor arrangements	7	Multi-stage loading
4	Model pile Installation	8	Bearing characteristics comparison of different foundations

mm, and the pile spacing is 3-6 times the pile diameter (D). So in this test, the pile spacing is set to be 219 mm, being about $3D$. In the case of equilateral triangle arrangement, the diameter of the reinforced area by single pile is 1.05 times the pile spacing, so it is about 230 mm. The model box is a closed box with a top opening, and the size of the box is 1000 mm×1000 mm×1200 mm (Fig. 5(a)), the data acquisition and control system are shown in Fig. 5(a). To avoid the boundary effects, the similarity ratio is set to be 1/5, and the diameter of the model pile is 70 mm ($D=70$ mm). After being maintained in standard condition for 28 days, the model pile is shown in Figs. 5(b) and 5(c).

To acquire the bearing characteristics of pervious concrete piles in soft soil foundations, two kinds of soil (silt and clay) were considered. The silt was taken from Yancheng City, and the clay was obtained from the highway construction site in Yixing City, they are all in eastern China. Figs. 6(a) and 6(b) show the grain-size distribution of silt and clay, and Table 6 are the parameters.

During the test, the pressure sensors, strain gauges and settlement sensors were arranged to acquire the bearing characteristics of the composite foundation, as Figs. 5 and 7 show. The steel loading plate is 230 mm in diameter, and two pressure sensors (1# and 2# in Fig. 7(a)) were arranged on the pile top symmetrically to acquire the pile stress, which can balance the stiffness difference during loading. Below the cushion, one pressure sensor (3#) was installed at a distance of $1D$ from the pile center, and it was set for the soil stress (Figs. 7(a) and 7(b)).

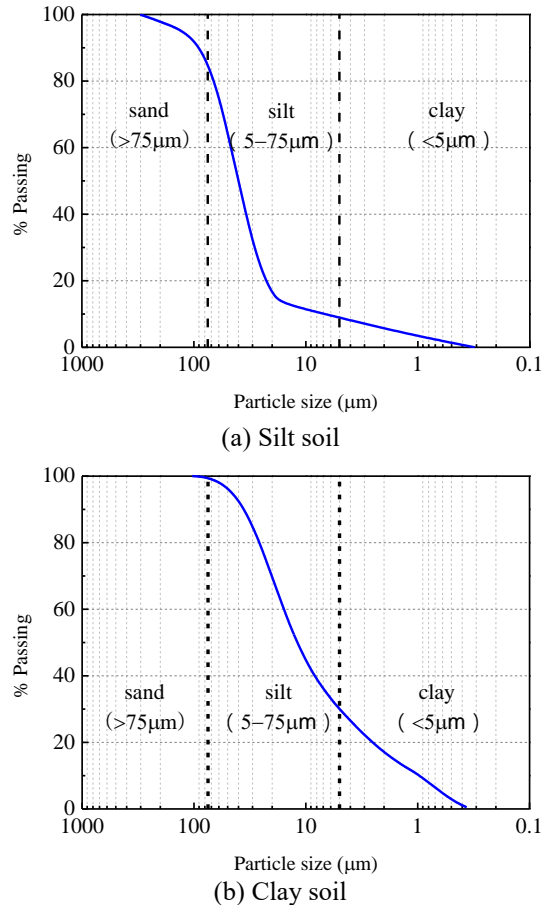


Fig. 6 Grain-size distribution of the soil

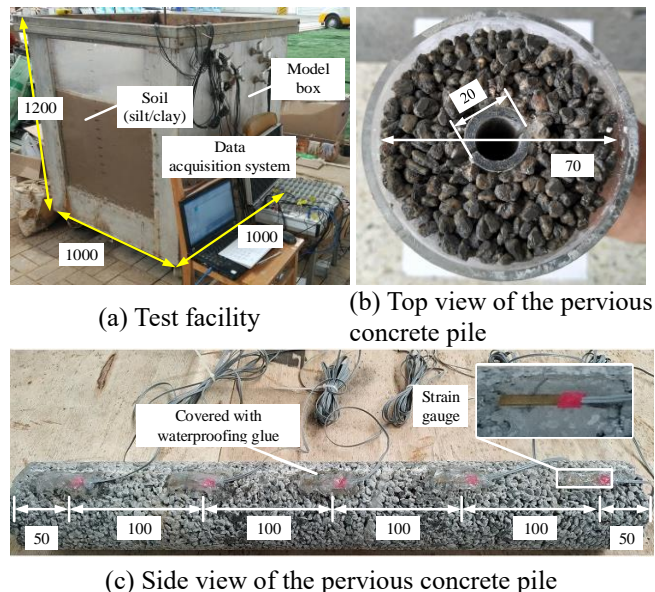


Fig. 5 Test facility and model pile (Unit: mm)

Table 6 Parameters of soil

Soil	Liquid limit w_L (%)	Plastic limit w_P (%)	Plastic index I_P	Natural density ρ_n (g/cm ³)	Specific gravity G_s (g/cm ³)
Silt	32.8	24.4	8.4	1.79	2.74
Clay	35.6	19.5	16.1	1.91	2.72

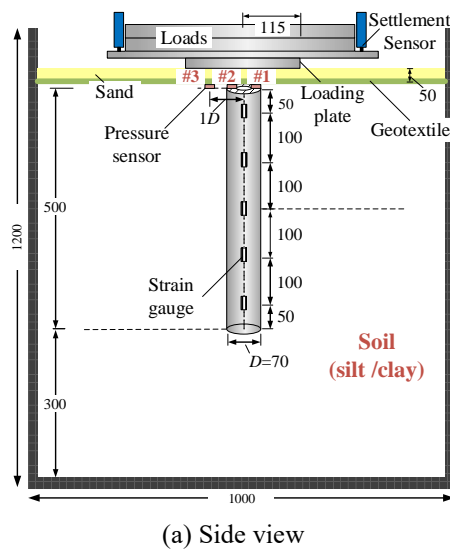
Table 7 Parameters for the soil in the model box

Soil	Density ρ (g/cm ³)	Dry density ρ_r (g/cm ³)	Water content w (%)	Void ratio e	Saturation S_r (%)
Silt	1.919	1.482	29.5	0.849	95.2
Clay	2.020	1.530	32.1	0.910	95.9

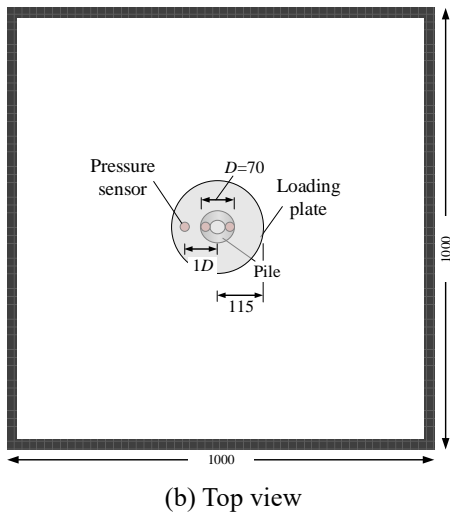
For the large quantity of soil needed in the model test, according to the research of Chen *et al.* (2013) and Zhao *et al.* (2017), the soil was filled by layers, with the thickness of each layer being 100 mm. Firstly, according to the designed water content, weigh the mass of soil needed for each layer, and add water to make it the slurry with the designed water content. After being mixed thoroughly, the slurry was filled in the model box and being static for over 12 hours (or being rammed to the specified height). During the test, the model box was covered with plastic film to prevent evaporation. After filling each layer, the soil was sampled with a cutting ring and tested for the satisfaction of requirements. After filling to the height of 800 mm, the model box was placed for at least 7 days until the excess pore water pressure in the soil dissipated. The parameters of the soil in the box are shown in Table 7.

3.2 Loading sequence

According to the technical code of DB37/T 5214-2018, the thickness of the cushion should be determined



(a) Side view



(b) Top view

Fig. 7 Instrumentation for the model test (Unit: mm)

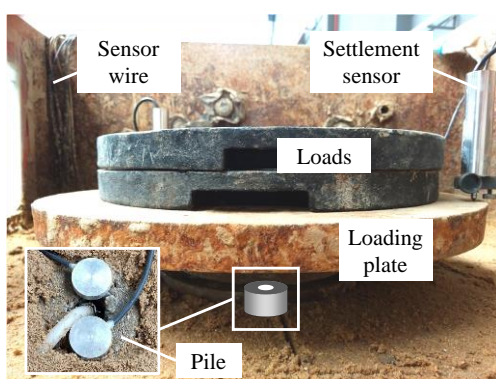


Fig. 8 Loading procedure

by the replacement ratio and the properties of the soil between piles, and the recommended thickness can be 150-300 mm for the in-site application. More load can be shared by the foundation soil with a thicker cushion layer (Madhav and Sharma 2009). In this test, the foundation soil with high water content is prepared, so the upward penetration of the pile may be larger, and the similarity ratio is set to be 1/5,

the thickness of cushion in the model test can be 50 mm (Fig. 8). After pile installation, the geotextile and coarse sand were placed on the foundation as the cushion. According to the technical code of GB/T 50783-2012 for composite foundation, the slow load keeping method was applied in the loading procedure, as Fig. 8 shows. 5%-10% of the maximum load was used for the preloading, after that, unloaded the loads and the formal test started. During the test, when the settlement slowed down and stabilized, the next stage of load can be continued. Also according to the technical code of GB/T 50783-2012, the load in each stage is 400 N, when the relative settlement in the loading test reaches 0.1, the test can be terminated, so the maximum loads in silty and clay foundations can be 4800 N and 4400 N, respectively.

4. Test results

Figs. 9(a) and 9(b) are the pervious concrete piles after performing the test, and the pile surface and pores were covered with soil particles, it is the water carried the soil into the pores during the drainage process. In Fig. 9(b), after the drainage process, the pervious concrete pile in the clay foundation is surrounded by a thick layer of clay, which may lead to the declination of pile permeability.

4.1 Bearing characteristics of foundations

Fig. 10 presents the measured load-settlement responses of the two foundations. With load increases, the settlement of the two foundations increases gradually. According to the technical code of GB/T 50783-2012 for composite foundation, the characteristic value of bearing capacity of composite foundation can be determined by relative settlement ratio. And it means that when the ratio of settlement to loading plate diameter reaches 0.01, the load is the characteristic value of bearing capacity. In this test, the relative settlement ratio can be 0.01, and the diameter of the loading plate is 230 mm, so the settlement of this value is 2.3 mm. In Fig. 10, the characteristic values of bearing capacity of the silty foundation and clay foundation can be 58 kPa and 50 kPa, respectively. So the bearing capacity of the silty foundation is 16% higher than that of the clay foundation, the reinforcement effect of the silty foundation with pervious concrete pile is slightly better than that of the clay foundation.

The process of pile-soil stress ratio variation can be the stress redistribution from the cushion, and the stress ratio of pile to soil is needed to evaluate the pile efficiency of the composite foundation. Figs. 11(a) and 11(b) illustrate the pile-soil stress ratios with time in the two foundations. At the moment of each load, an obvious rising of the pile-soil stress ratio appears, then it gradually falls and tends to be stable.

It is the larger stiffness of pile than that of the soil, and more loads were shared by the pile when the load is added, the pile-soil stress ratio increases rapidly. With the consolidation of soil around the pile and the adjustment of the cushion, the pile-soil stress ratio gradually decreases and becomes stable (Han *et al.* 1993, Cao *et al.* 2008). The permeability coefficient of clay is significantly lower than

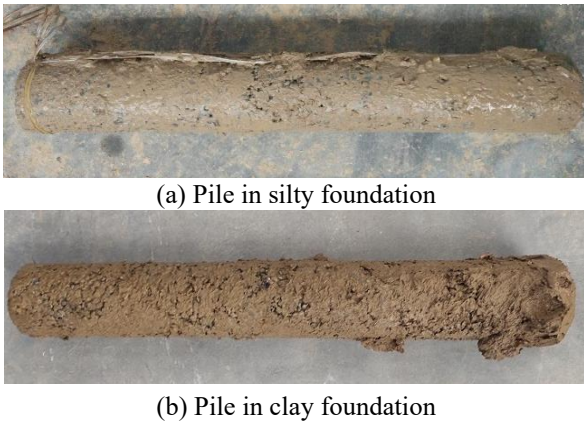


Fig. 9 Pervious concrete piles after performing loading test

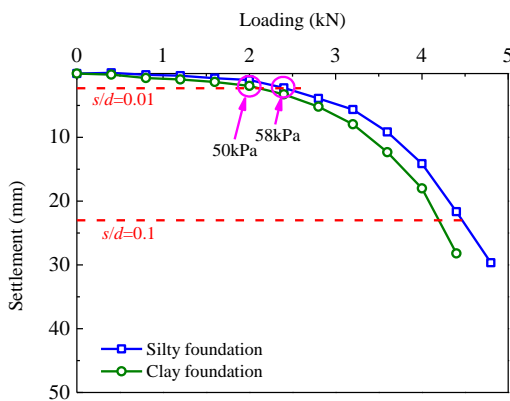


Fig. 10 Load-settlement response for silty and clay foundations

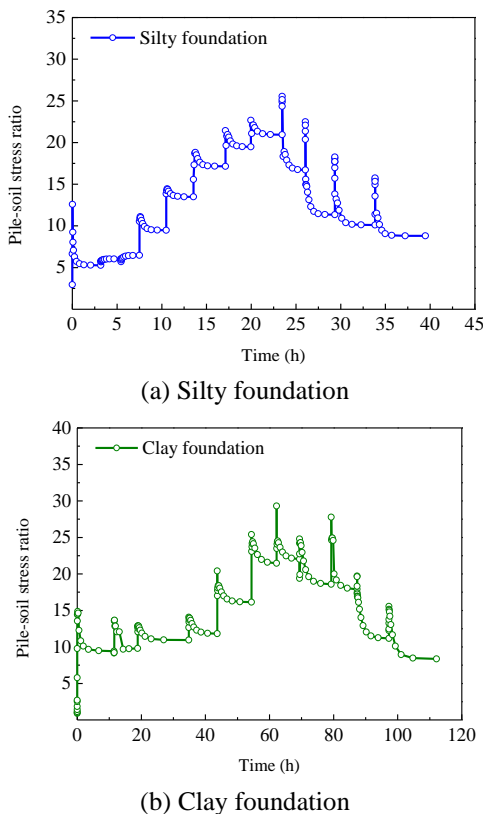


Fig. 11 Relationship between pile-soil stress ratio and time

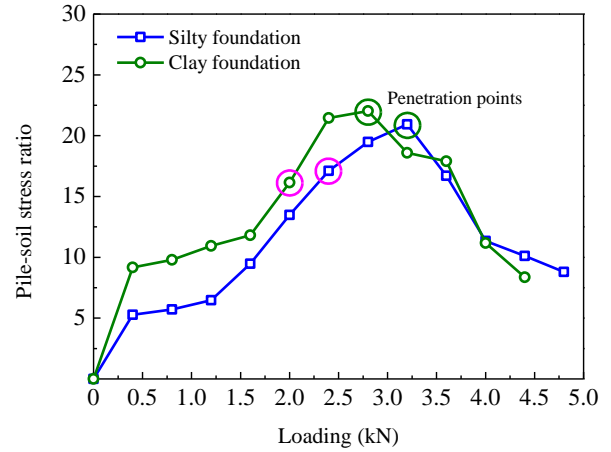


Fig. 12 Relationship between pile-soil stress ratio and loading

that of silt, so more time was needed for the stabilization. Besides, further comparisons of pile-soil stress ratios between the two foundations were available in Fig. 12, and it is the relationship between pile-soil stress ratio and loading.

In Fig. 12, the pile-soil stress ratios of the two foundations both increase first and then decrease with the applied loads. At the beginning of loading, in the initial stage, the pile-soil stress ratio is relatively small, with the increase of the load and the consolidation of the soil, the settlement of the foundation soil is obviously greater than that of the pile, so the pile top penetrates into the cushion, which can increase the pile-soil stress ratio to a certain degree. For the low bearing capacity of clay, less load was shared by the foundation soil, so the pile-soil stress ratio of the clay foundation can be larger at the early stage of the test. For the later period of the test, more load was shared by the pile, the settlement of the pile becomes larger, leading to a smaller differential settlement of the pile and soil, which is also illustrated by Ko *et al.* (2018). At the same time, the pile moves downward under the load, and the foundation soil shares more loads through the cushion, so the pile-soil stress ratio gradually decreases in this process.

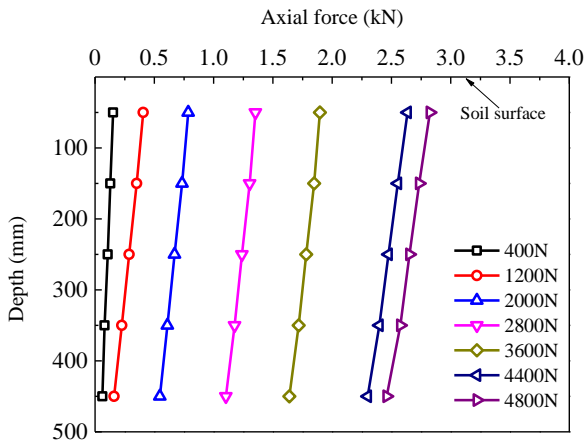
4.2 Bearing characteristics of piles

By sticking strain gauges along the pile depth (Fig. 5), strain distributions of the pile can be obtained. So the pile axial force at the measured depth (Q_z) in the model pile can be calculated as

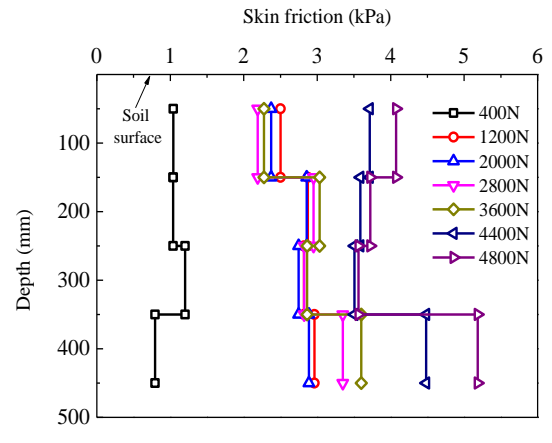
$$Q_z = E\varepsilon A \quad (3)$$

Where E is the elastic modulus of the pervious concrete pile when porosity is 30%, and it is 20 GPa, ε is the strain of the pile at the designed section, A is the cross-sectional area of the pile.

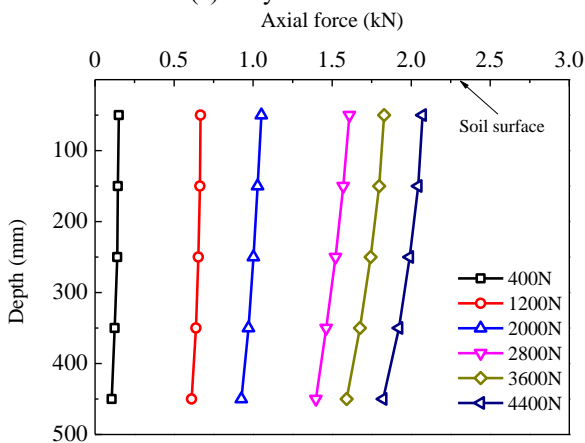
The pile axial force distributions of the two foundations are in Fig. 13. It shows that the axial forces increase with the applied loads, but decrease with depth due to the skin friction. In the initial stage (400 N), the axial forces in the two foundations along the pile length are almost the same.



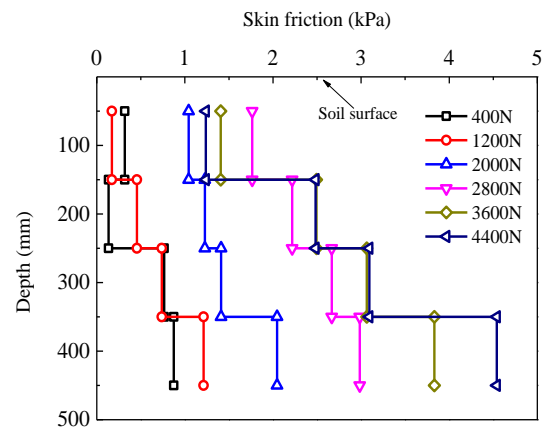
(a) Silty foundation



(a) Silty foundation



(b) Clay foundation



(b) Clay foundation

Fig. 13 Distribution of the axial force under different loads

Fig. 15 Distribution of the skin friction under different foundations

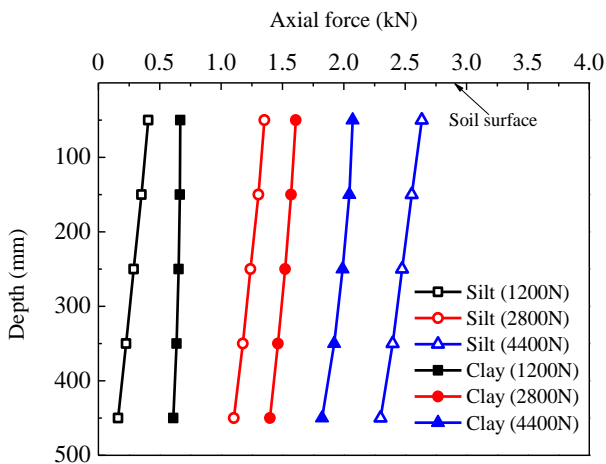


Fig. 14 Comparison of the axial force under different loads

show that, when it is less than 2800 N, the axial force of silty foundation is smaller than that of the clay foundation, it can be the silty foundation with higher bearing capacity shares more loads, so the loads shared by pile and the axial force are less. Besides larger consolidation settlement of clay soil results in the upward penetration of pile into the cushion, which also leads to the increase of load shared by pile. Combined with the result of Fig. 12, the pile penetrates downward to the underlying soft layer, and the load is transferred from pile to soil, so during the later period of the test (2800-4400 N), the axial force of the pile in the silty foundation becomes larger. This may be the higher bearing capacity of the pile in the silty foundation and the less downward penetration to the underlying layer.

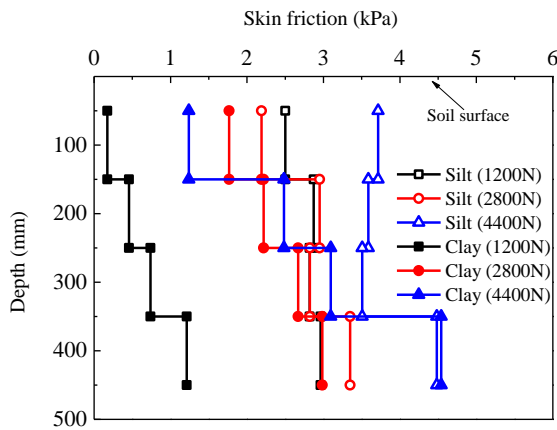
Increasing the loads, the pile axial force at each loading stage for silty foundation is smaller than that of the clay foundation at 400-2800 N, and it means less loads were shared by the pile in the silty foundation, which is in consistent with the results of Fig. 12.

When the pile tip is located in soft soil, the bearing capacity of a pile is mainly provided by the skin friction, and it can be essential for its design and analysis (Wu *et al.* 2015). The skin friction distribution along the pile depth can be acquired by Eq. (4)

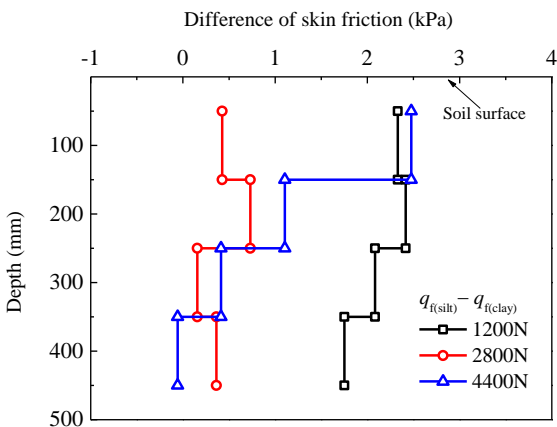
For comparative analysis, the pile axial forces of silty and clay foundations are plotted in Fig. 14. The results

$$q_s = \frac{Q_2 - Q_1}{\pi D \Delta L} \quad (4)$$

Where Q_1 and Q_2 are the axial forces of the two adjacent cross-sections, D is the diameter of pile, ΔL is the length between the two cross-sections. Fig. 15 presents the



(a) Skin friction distribution



(b) Skin friction difference

Fig. 16 Comparisons of skin friction along depth

distribution of skin friction along the pile depth in silty and clay foundations. Results show that the skin friction generally increases with the applied loads, and for the clay foundation, the skin friction almost increases with the pile depth, but the same pattern did not appear in the silty foundation. It means that the skin friction of the pile in the clay foundation is more affected by the lateral stress. While in the silty foundation, for the higher consolidation efficiency, the skin friction is greatly affected by the effective stress of foundation soil, and the skin friction on the upper part of the pile can be greater. Therefore, the skin friction of piles in the two foundations presents different distribution along pile depth. In Fig. 15(a), for the pile in the silty foundation, a large increase of skin friction appears during the load of 400-1200 N. While in the clay foundation, the skin friction increases slowly with the applied loads for the lower consolidation efficiency, so the increase of skin friction in clay is not so obvious.

Besides, the skin friction reflects the relative slip between pile and soil, for common end bearing piles, due to the high tip resistance, deformation mainly occurs on the upper part. But for the pervious concrete piles with tips in soft soil, which are designed for the frictional piles, without the support from the pile tip, the piles will move downward as a whole, so the distribution of skin friction is different from common end bearing piles.

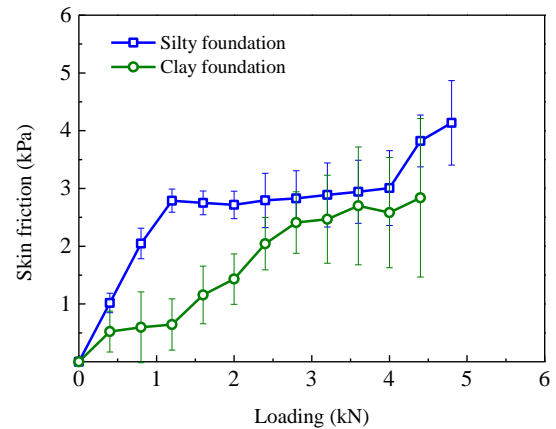


Fig. 17 Comparison of the skin friction under different loads

Also, the comparison of skin friction between silty and clay foundations is illustrated in Fig. 16(a), the skin friction of pile in the silty foundation is larger than that of the clay foundation generally, and the difference of the skin friction between piles are available in Fig. 16(b). Except for the bottom at the load of 4400 N, the skin friction of pile in the silty foundation is larger than that of the clay foundation, especially for the upper portion of the pile, the skin friction advantage is more obvious. For the two foundations, at the load of 4400 N and on the pile top (50-150 mm), the maximum difference is 2.48 kPa.

The bearing capacity of the pile increases with the dissipation of excess pore water pressure and time (Fattah *et al.* 2013), and the pile bearing capacity is composed of pile tip resistance and skin friction. The average value and standard deviation were calculated by the skin friction of different parts on the pile, and the results are illustrated in Fig. 17. The average skin friction in the silty foundation increases significantly faster than that of clay foundation, and the difference is even more obvious in the early stage of loading. With the increase of load, the skin friction of the pile in silty soil gradually slows down, it may be that more loads were shared by the foundation soil at this time. And the skin friction of the pile in clay foundation increases slowly, but still increases with the applied loads. Then at the load of 4400 N, the average skin friction of the pile in the silty foundation is 3.82 kPa, and for the clay foundation it is 2.84 kPa, so the skin friction of the pile in the silty foundation is about 35% higher.

5. Conclusions

To investigate the bearing characteristics of the pervious concrete pile composite foundation in soft soils, the pervious concrete piles were applied in silty and clay foundations for comparison, and the settlement, the pile-soil stress ratio and the skin friction during the multi-stage loading were obtained, the conclusions are as follows:

- Based on the strength and permeability results of pervious concrete with different aggregate sizes (3-5 mm and 4-6 mm) and porosities (20%, 25%, 30% and

35%), the recommended aggregate size for pervious concrete can be 3-5 mm, and the porosity is 30%.

- According to the load-settlement response for silty and clay foundations, the characteristic value of bearing capacity can be achieved when the relative settlement ratio is 0.01. Results show that the bearing capacity of the silty foundation is 16% higher than that of the clay foundation.
- The pile-soil stress ratios of the two foundations both increase first and then decrease with the applied loads. For the silty foundation, in the early stage of loading, the pile-soil stress ratio is smaller for the faster consolidation rate and higher bearing capacity. But when it is the ultimate load for the pile, it will penetrate into the underlying layer, and the pile-soil stress ratio decreases.
- The pile axial force distributions of the two foundations show that the axial force increases with the applied loads, but decreases with depth for the skin friction. For the higher skin friction of the pile in the silty foundation, the pile penetration into the underlying layer is smaller, so the reduction of axial force of the pile in the silty foundation can be lower.
- The skin friction of the two foundations both increases with the load. For the consolidation efficiency difference in different soils, the skin friction is greatly affected by the soil effective stress in the silty foundation, while the skin friction of pile in clay foundation is more affected by the lateral stress. At the load of 4400 N, the skin friction of the pile in silty foundation is about 35% higher than that of the clay foundation.

References

- ACI 522R (2010), Report on Pervious Concrete, American Concrete Institute, Farmington Hills, MI, USA.
- Ahn, J. and Kim, Y. (2012), "Consolidation behavior and stress concentration ratio of SCP composite ground", *Mar. Georesour. Geotechnol.*, **30**(1), 63-85. <https://doi.org/10.1080/1064119X.2011.586011>.
- Alamgir, M.N., Miura, H.B. Poorooshasb and Madhav, M.R. (1996), "Deformation analysis of soft ground reinforced by columnar inclusions", *Comput. Geotech.*, **18**(4), 267-299. [https://doi.org/10.1016/0266-352X\(95\)00034-8](https://doi.org/10.1016/0266-352X(95)00034-8)
- Andreou, P., Frikha W., Frank R., Canou J., Papadopoulos V. and Dupla J.C. (2008), "Experimental study on sand and gravel columns in clay", *Proc. Inst. Civ. Eng. Ground Improv.*, **161**(4), 189-198.
- ASTM. (1974), "Standard method of test for permeability of granular soils (constant head)", D2434-74.
- Baez, J.I. (1995), "A design model for the reduction of soil liquefaction by vibro-stone columns", Ph.D. dissertation, Univ. of Southern California, Los Angeles.
- Barksdale, R.D. and Bachus, R.C. (1983), "Design and construction of stone columns", *FHWA/RD 83/026, Rep. No. 1, Vol. 1*, Federal Highway Administration (FHWA), Washington, DC.
- Cao, W.P., Chen, Y.M. and Chen, R.P. (2008), "Analysis of soil arching in piled embankments considering coupled effect of embankment filling and soil consolidation", *Chinese J. Rock Mech. Eng.*, **27**(8), 1610-1617.
- Chen, J. Sheng, Q. Liu, X.M. Zhu, Z.Q., Leng, X.L. Zhang, Y.H. and Chen, G.L. (2013), "An production method of solid model layered tamping for the pseudo-earth- quake shaking table test". Chinese patent No.201310154909.8, Institute of Rock and Soil Mechanics, Chinese Academy of Sciences, Wuhan, China.
- CJJ/T 135-2009 (2009), Technical specification for pervious cement concrete pavement, Ministry of housing and urban-rural development of the people's republic of China, China Architecture & Building Press, Beijing, China.
- Cui, X.Z., Wang, C., Zhou, Y.X., Zhang, N. and Gao, Z.J. (2012), "Anti-earthquake mechanism of pervious concrete pile composite foundation", *J. Shandong Univ., Eng. Sci.*, **42**(4), 86-91. [https://doi.org/10.1672-3961\(2012\)04-0086-06](https://doi.org/10.1672-3961(2012)04-0086-06).
- Cui, X.Z., Zhang, J., Chen, D.H., Li, S.C., Jin, Q., Zheng, Y.J. and Cui, S.Q. (2018), "Clogging of pervious concrete pile caused by soil piping an approximate experimental study", *Can. Geotech. J.*, **55**, 999-1015. <https://doi.org/10.1139/cgj-2017-0238>.
- Das, B.M. (2010), *Principles of geotechnical engineering* (7th Ed.), Wadsworth Inc., 683.
- Fattah, Mohammed Y., Al-Mosawi, Mosa J. and Al-Zayadi, Abbas A.O. (2013), "Time dependent behavior of piled raft foundation in clayey soil", *Geomech. Eng.*, **5**(1), 17-36. <https://doi.org/10.12989/gae.2013.5.1.017>.
- GB/T 50783-2012 (2012), Technical code for composite foundation, Ministry of housing and urban-rural development of the people's republic of China, China Planning Press, Beijing, China.
- Ghafoori, N. and Dutta, S. (1995), "Laboratory investigation of compacted no-fines concrete for paving materials", *J. Mater. Civil Eng.*, **7**(3), 183-191.
- Han, J., Ye, S.L. and Zhang, D.S. (1993), "In-situ observations on back-pressures and pore water pressures in composite foundation with stone columns", *Chinese J. Geotech. Eng.*, **15**(5), 40-47.
- Housing and urban-rural development department of Shandong province (2018), "Technical code for composite foundation of pervious concrete pile", DB37/T 5214-2018, China Building Materials Press, Beijing, China.
- Huang, B.S., Wu, H., Shu, X. and Burdette, E.G. (2010), "Laboratory evaluation of permeability and strength of polymer-modified pervious concrete", *Constr. Build. Mater.*, **24**(5), 818-823. <https://doi.org/10.1016/j.conbuildmat.2009.10.025>.
- Ko, J., Cho, J. and Jeong, S. (2018), "Analysis of load sharing characteristics for a piled raft foundation", *Geomech. Eng.*, **16**(4), 449-461. <https://doi.org/10.12989/gae.2018.16.4.449>.
- Kwon, J., Kim, C., Im, J.C. and Yoo, J.W. (2018), "Effect of performance method of sand compaction piles on the mechanical behavior of reinforced soft clay", *Geomech. Eng.*, **14**(2), 175-185. <https://doi.org/10.12989/gae.2018.14.2.175>.
- Madhav, M.R. and Sharma, J.K. (2009), "Settlement of and load distribution in a granular piled raft", *Geomech. Eng.*, **1**(1), 97-112. <https://doi.org/10.12989/gae.2009.1.1.097>.
- Malaiskiene, J., Kizinievic, O and Sarkauskas, A (2020), "The impact of coarse aggregate content on infiltration rate, structure and other physical & mechanical properties of pervious concrete", *Eur. J. Environ. Civ. Eng.*, **24**(5), 569-582. <https://doi.org/10.1080/19648189.2017.1410231>.
- Mitchell, J. K. (1981), "State-of-the-art report, session 12", *Proc., 10th Int. Conf. on Soil Mechanics and Foundation Engineering*, Balkema, Rotterdam, Netherlands, 506-565.
- Neithalath, N., Sumanasooriya, M.S. and Deo, O. (2010), "Characterizing pore volume, sizes, and connectivity in pervious concretes for permeability prediction", *Mater. Charact.*, **61**(8), 802-813. <https://doi.org/10.1016/j.matchar.2010.05.004>.
- Nguyen, D.H., Sebaibi, N., Boutouil, M., Leleyter, L. and Baraud,

- F. (2014), "A modified method for the design of pervious concrete mix", *Constr. Build. Mater.*, **73**, 271-282. <https://doi.org/10.1016/j.conbuildmat.2014.09.088>.
- Ni, L.S., Suleiman, M.T. and Raich, A. (2016), "Behavior and soil-structure interaction of pervious concrete ground-improvement piles under lateral loading", *J. Geotech. Geoenviron. Eng.*, **142**(2), 04015071. [https://doi.org/10.1061/\(ASCE\)GT.1943-5606.0001393](https://doi.org/10.1061/(ASCE)GT.1943-5606.0001393).
- Okamura, M., Ishihara, M. and Tamura, K. (2006). "Degree of saturation and liquefaction resistances of sand improved with sand compaction pile", *J. Geotech. Geoenviron. Eng.*, **132**(2), 258-264. [https://doi.org/10.1061/\(ASCE\)1090-0241\(2006\)132:2\(258\)](https://doi.org/10.1061/(ASCE)1090-0241(2006)132:2(258)).
- Qin, Y.H., Liang, J., Yang, H.F. and Deng, Z.H. (2016), "Gas permeability of pervious concrete and its implications on the application of pervious pavements", *Measurement*, **78**, 104-110.
- Schokker, A. J. (2010), "The sustainable concrete guide: strategies and examples", US Green Concrete Council.
- Suleiman, M.T., Ni, L.S. and Raich, A. (2014), "Development of pervious concrete pile ground-improvement alternative and behavior under vertical loading", *J. Geotech. Geoenviron. Eng.*, **140**(7), 04014035. [https://doi.org/10.1061/\(ASCE\)GT.1943-5606.0001135](https://doi.org/10.1061/(ASCE)GT.1943-5606.0001135).
- Tao, Z.H. (2006), "Research on material design and performance of porous cement concrete pavement", Ph.D. Dissertation, Southeast University. Nanjing
- Tennis, P.D., Leming, M.L. and Akers, D.J. (2004), "Pervious Concrete Pavements (No. PCA Serial No. 2828)", Portland Cement Association, Skokie, Illinois
- Wu, Y.D., Liu, J. and Chen, R. (2015). "An analytical analysis of a single axially-loaded pile using a nonlinear softening model". *Geomech. Eng.*, **8**(6), 769-781. <https://doi.org/10.12989/gae.2015.8.6.769>.
- Yahia, A. and Kabagire, K.D. (2014), "New approach to proportion pervious concrete", *Constr. Build. Mater.*, **62**, 38-46. <https://doi.org/10.1016/j.conbuildmat.2014.03.025>
- Yu, Y., Wang, Z. and Sun, H.Y. (2020) "Optimal design of stone columns reinforced soft clay foundation considering design robustness", *Geomech. Eng.*, **22**(4), 305-318. <https://doi.org/10.12989/gae.2020.22.4.305>.
- Zhang, J., Cui, X.Z., Huang, D., Jin, Q., Lou, J.J. and Tang, W.Z. (2016), "Numerical simulation of consolidation settlement of pervious concrete pile composite foundation under road embankment", *Int. J. Geomech.*, **16**(1), B4015006. [https://doi.org/10.1061/\(ASCE\)GM.1943-5622.0000542](https://doi.org/10.1061/(ASCE)GM.1943-5622.0000542).
- Zhang, N., Cui, X.Z., Zhang, J., Zhou, Y.X., Gao, Z.J. and Sui, W. (2013), "Settlement-controlling and pressure-reduction effect of pervious concrete pile under the action of embankment load", *J. Shandong Univ., Eng. Sci.*, **43**(4), 80-86. <https://doi.org/10.6040/j.issn.1672-3961.0.2013.088>.
- Zhang, X.F., Li, Q.N., Ma, Y., Zhang, X.J. and Yang, S.Z. (2014), "Large-scale pilot test study on bearing capacity of sea-crossing bridge main pier pile foundations", *Geomech. Eng.*, **7**(2), 201-212. <https://doi.org/10.12989/gae.2014.7.2.201>.
- Zhao, F., Hu, H.S., Yang, G.S. and Hou, M.X. (2017), "Development of the model box design and soil sample preparation technology for pile-soil model test", *Low Temperature Architect. Technol.*, **39**(7), 66-70.